Journal of ELECTRONIC MATERIALS, Vol. 47, No. 1, 2018
DOI: 10.1007/s11664-017-5808-y


# Influence of $Y_2O_3$ Addition on Crystallization, Thermal, Mechanical, and Electrical Properties of $BaO$-$Al_2O_3$-$B_2O_3$-$SiO_2$ Glass–Ceramic for Ceramic Ball Grid Array Package

BO LI,[1,2,3,4] WEI LI,[1] and JINGGUO ZHENG[1]

1.—School of Microelectronics and Solid-State Electronics, University of Electronic Science and Technology of China, Chengdu 610054, China. 2.—State Key Laboratory of Electronic Thin Films and Integrated Devices, Chengdu 610054, China. 3.—National Engineering Research Center of Electromagnetic Radiation Control Materials, Chengdu 610054, China. 4.—e-mail: boli@uestc.edu.cn

$Y_2O_3$ addition has a significant influence on the crystallization, thermal, mechanical, and electrical properties of $BaO$-$Al_2O_3$-$B_2O_3$-$SiO_2$ (BABS) glass–ceramics. Semi-quantitative calculation based on x-ray diffraction demonstrated that with increasing $Y_2O_3$ content, both the crystallinity and the phase content of cristobalite gradually decreased. It is effective for the additive $Y_2O_3$ to inhibit the formation of cristobalite phase with a large coefficient of thermal expansion value. The flexural strength and the Young's modulus, thus, are remarkably increased from 140 MPa to 200 MPa and 56.5 GPa to 63.7 GPa, respectively. Also, the sintering kinetics of BABS glass–ceramics with various $Y_2O_3$ were investigated using the isothermal sintering shrinkage curve at different sintering temperatures. The sintering activation energy $Q$ sharply decreased from 99.8 kJ/mol to 81.5 kJ/mol when 0.2% $Y_2O_3$ was added, which indicated that a small amount of $Y_2O_3$ could effectively promote the sintering procedure of BABS glass–ceramics.

**Key words:** CBGA package, glass–ceramic, thermal properties, sintering kinetics

## INTRODUCTION

At present, low temperature co-fired ceramic (LTCC) technology plays a very crucial role in microwave integrated circuits, radio frequency devices, etc., which have been enormously employed in the modern wireless communication technologies.[1–4] As the requirement of high packing density, high signal propagation speed, and high-reliability packages, microelectronic packaging materials should possess good dielectric properties (low permittivity and low loss), and excellent mechanical properties (high flexural strength and Young's modulus). Moreover, with regard to the ceramic ball grid array (CBGA) package, a high coefficient of thermal expansion (CTE) is required to relieve the thermal mismatch between the substrate and the printed circuit board (PCB) with a CTE value 12–18 $\times$ $10^{-6}$/°C.[5–7]

Currently, barium aluminum borosilicate glass–ceramics have been extensively reported owing to low dielectric constant and loss, as well as high CTE value. Actually, Lim et al.[8,9] studied the effect of BaO and $Al_2O_3$ content on the dielectric, sintering behavior, and physical properties of $BaO$-$B_2O_3$-$SiO_2$ glass. Chen et al.[10] found that $BaO$-$B_2O_3$-$SiO_2$ system had high coefficients of thermal expansion (11–17 $\times$ $10^{-6}$/°C), low permittivity (7.1–7.4), and low loss (5–7 $\times$ $10^{-4}$). And Borhan et al.[11] reported the influence of additives CoO, CaO, and $B_2O_3$ on $BaO$-$Al_2O_3$-$SiO_2$ glass and found $B_2O_3$-rich compositions exhibited excellent thermal stability. Therefore, the above researches indicate that a new quaternary system, $BaO$-$Al_2O_3$-$B_2O_3$-$SiO_2$ (BABS)

(Received May 12, 2017; accepted September 13, 2017; published online October 20, 2017)

glass–ceramic, may have a great potential for LTCC applications such as CBGA packages.

Some researchers have studied the effect of $Y_2O_3$ addition on other systems, e.g., $MgO$-$Al_2O_3$-$B_2O_3$-$SiO_2$ glass,[12] $SrO$-$B_2O_3$-$SiO_2$ glass,[13] and $BaO$-$B_2O_3$-$SiO_2$ glass.[14] However, the influence of $Y_2O_3$ on the $BaO$-$Al_2O_3$-$B_2O_3$-$SiO_2$ system has not yet been reported. In this work, the effect of $Y_2O_3$ addition on crystallization, thermal, mechanical, and electrical properties of BABS glass–ceramics was investigated. Also, the thermal expansion characteristic was further analyzed based upon the modified equations. In order to understand the role of $Y_2O_3$ addition on the sintering behavior of BABS glass–ceramics, the sintering kinetics based on the isothermal sintering shrinkage curves at different sintering temperatures was also researched.

## EXPERIMENTAL PROCEDURE

The chemical compositions of the $BaO$-$Al_2O_3$-$B_2O_3$-$SiO_2$ glass–ceramic are listed in Table I. Analytical reagent grades of $Ba(OH)_2$, $Al(OH)_3$, $H_3BO_3$, $H_3SiO_3$, and $Y_2O_3$ were used as raw materials. The weighed powders were ball-milled with zirconia balls for 7 h using deionized water as medium, and then dried completely. After calcination at 700°C for 3 h, the prepared powders mixed with acrylic acid as organic binder were pressed to bars (50 mm × 4 mm × 3 mm) and disks (15 mm × 1 mm) under a pressure of 25 MPa. These green compacts were sintered at 880°C, 900°C, and 920°C in air.

The glass–ceramics were pulverized into powder, and then the crystal structures were measured by an x-ray diffractometer (XRD, PANALYTICAL PW3040/60) using Cu K$\alpha$ radiation in the $2\theta$ between 20° and 70° in a sampling interval of 0.02°. The whole pattern fitting method was used for the semi-quantitative calculation of the phase content and the crystallinity based on the XRD pattern. The microstructures of samples were analyzed by a scanning electron microscopy (SEM, FEI INSPECT F50). The sintering kinetic parameters were evaluated by using a dilatometer (NETZSCH DIL 402 PC). Also, to obtain the coefficient of thermal expansion (CTE), the thermal expansion behavior of fired samples was carried out at a heating rate of 3°C/min from 25°C to 600°C using a dilatometer (NETZSCH DIL 402 PC). The dielectric properties (including $\varepsilon_r$ and $\tan\delta$ at 1 MHz) of samples were tested by a precision LCR meter (Agilent 4284A). In addition, the flexural strength and the Young's modulus of the specimens were measured via the three-point method by an electronic universal testing machine (MTS SANS CMT-6104).

## RESULTS AND DISCUSSION

In order to explore the effect of $Y_2O_3$ content on the crystalline phase, the XRD patterns of BABS glass–ceramics containing various amounts of $Y_2O_3$ sintered at 920°C are shown in Fig. 1. It appears that all samples exhibit the diffraction peaks belonging to quartz and cristobalite. Apparently, the major crystal phase is quartz (JCPDS no. 70-3755) and the minor crystal phase is cristobalite (JCPDS no. 77-1317). It can be observed that the intensity of the diffraction peak at 22°, corresponding to cristobalite phase, gradually decreases with the increase of $Y_2O_3$ content. Therefore, the amount of cristobalite decreased since the addition of $Y_2O_3$ inhibits the process of the formation of cristobalite. As shown in Table II, the semi-quantitative calculation of BABS glass–ceramics was estimated by MDI Jade 6 through the whole pattern fitting method with residual error less than 5%. With increasing $Y_2O_3$ content, the crystallinity of samples was gradually lowered from 38.79% to 27.85%. This result suggested that $Y_2O_3$ addition could restrain the crystallization of BABS glass–ceramics. Moreover, the phase content of quartz increased from 80.8 wt.% to 96.4 wt.%, but that of cristobalite decreased from 19.2 wt.% to 3.6 wt.%. Obviously, it is effective for the additive $Y_2O_3$ to inhibit the formation of cristobalite phase. Since the cristobalite phase would undergo a displacive phase transition, it could seriously deteriorate the mechanical and thermal properties of BABS glass–ceramics. According to the above analysis, it was revealed that $Y_2O_3$ addition can avoid the excessive occurrence of cristobalite, which is advantageous to obtain the sample with good characteristics.

Figure 2 shows the thermal expansion curves of BABS glass–ceramics with different amounts of $Y_2O_3$. As we know, the displacive phase transition between $\alpha$- and $\beta$-cristobalite within 180–270°C will produce the dramatic CTE change,[15] and, thus, induce a strong nonlinearity of the thermal

**Table I. Compositions of BABS glass–ceramics (wt.%)**

| | BaO | $Al_2O_3$ | $B_2O_3$ | $SiO_2$ | $Y_2O_3$ |
|---|---|---|---|---|---|
| Y1 | 35 | 5 | 10 | 50 | 0 |
| Y2 | 35 | 5 | 10 | 50 | 0.1 |
| Y3 | 35 | 5 | 10 | 50 | 0.2 |
| Y4 | 35 | 5 | 10 | 50 | 0.5 |
| Y5 | 35 | 5 | 10 | 50 | 1 |

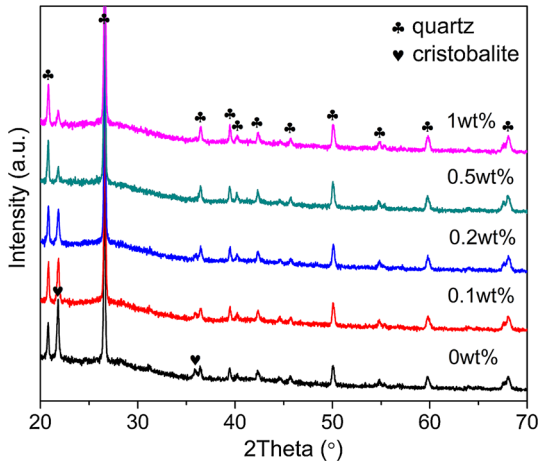


Fig. 1. XRD patterns of BABS glass–ceramics containing different $Y_2O_3$ content sintered at 920°C.

**Table II. Phase content and crystallinity of BABS glass–ceramics**

| | Phase content (wt.%) | | |
|---|---|---|---|
| **Designation** | **Quartz** | **Cristobalite** | **Crystallinity (%)** |
| Y1 | 80.8 | 19.2 | 38.79 |
| Y2 | 86.7 | 13.3 | 36.95 |
| Y3 | 88.5 | 11.5 | 35.13 |
| Y4 | 96.4 | 3.6 | 28.52 |
| Y5 | 96.1 | 3.9 | 27.85 |

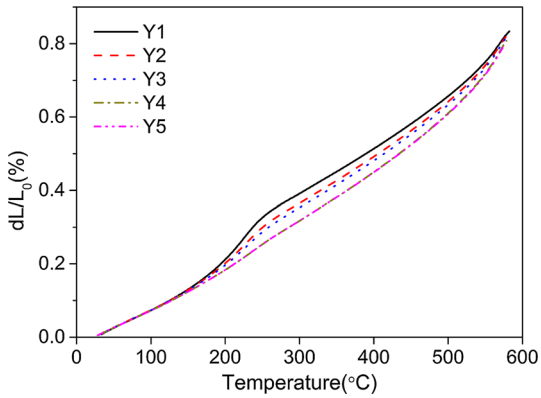


Fig. 2. Comparison of thermal expansion for the BABS glass–ceramics with various $Y_2O_3$ content sintered at 920°C.

expansion curve in this temperature range. Apparently, the variation of thermal expansion curves and CTE values is basically in agreement with the change of cristobalite content in BABS glass–ceramics. Therefore, the variation of cristobalite content and its displacive phase transition dominated the above changes about thermal behavior. Also, the CTE value in the temperature range of 20–300°C is

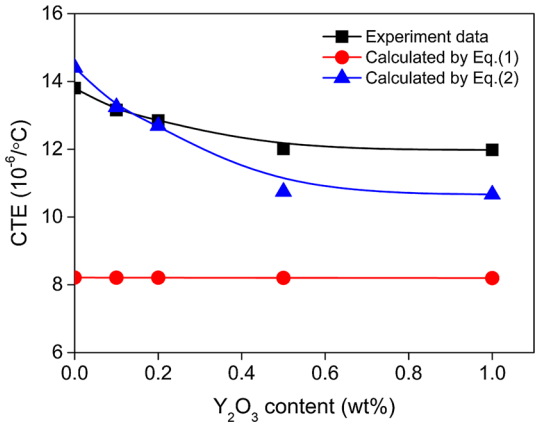


Fig. 3. Experimental and theoretical CTE values of BABS glass–ceramics versus $Y_2O_3$ content.

**Table III. The CTE values of oxides used for calculation**

| **Oxides** | **CTE ($10^{-6}$/°C)** | **Ref.** |
|---|---|---|
| BaO | 20 | 16 |
| $Al_2O_3$ | −4 | 16 |
| $B_2O_3$ | −4.07 | 16 |
| $SiO_2$ | 3.5 | 16 |
| $Y_2O_3$ | −2 | 16 |

drawn in Fig. 3. Usually, the CTE value of glass can be calculated through the CTE values of oxides in the glass network by the following formula.

$$\alpha = \sum_{i=1}^{n} \alpha_i x_i, \quad (1)$$

where $\alpha$ is the CTE value of glass, and $\alpha_i$ and $x_i$ is the CTE value and the mole fraction of the corresponding oxide species $i$, respectively. The CTE values of oxides (20–300°C) used for theoretical calculation are listed in Table III, and the calculated CTE values are illustrated in Fig. 3. Unfortunately, the calculated CTE values by Eq. 1 have a significant gap from the experimental dates, because the high CTE of crystal phase, such as cristobalite, was not taken into account. So we make a modified formula Eq. 2 to calculate the CTE value in this work.

$$\alpha = \alpha_g x_g + \sum_{i=1}^{n} \alpha_i x_i, \quad (2)$$

where $\alpha$ is the CTE value of glass–ceramic, $\alpha_g$ and $\alpha_i$ represents the CTE value of the residual glass phase and the crystal phase $i$, respectively. The $x_g$ and $x_i$ are the mass fraction of the residual glass phase and the crystal phase $i$. Additionally, $x_g$, $x_1$, $x_2$,… are calculated by the WPF method listed in

**Table IV. Electrical properties of BABS glass–ceramics with different amounts of $Y_2O_3$ sintered at 920°C**

| Electrical properties | Y1 | Y2 | Y3 | Y4 | Y5 |
|---|---|---|---|---|---|
| Dielectric constant | 6.1 | 6.3 | 6.5 | 6.8 | 6.8 |
| Dielectric loss ($\times 10^{-3}$) | 3.2 | 3.7 | 3.9 | 4.6 | 4.7 |
| Insulation resistivity (Ω cm) | $7.71 \times 10^{11}$ | $5.29 \times 10^{11}$ | $7.33 \times 10^{11}$ | $2.26 \times 10^{11}$ | $2.03 \times 10^{11}$ |

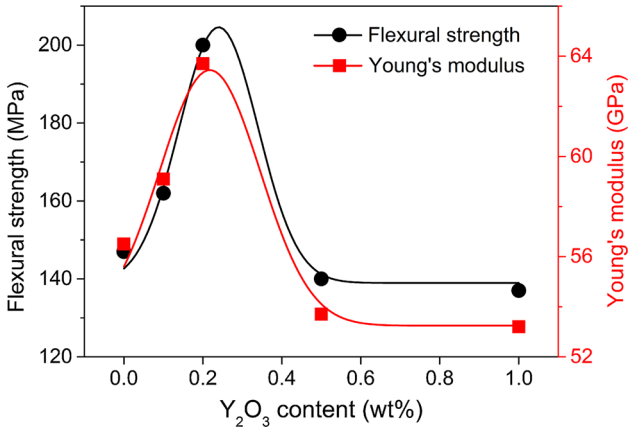


Fig. 4. Flexural strength and Young's modulus of BABS glass–ceramics with various amount of $Y_2O_3$ sintered at 920°C.

Table II. The CTE values of crystal phases (20–300°C) in this study are given below: α (quartz) = $13.2 \times 10^{-6}$/°C, α (cristobalite) = $50 \times 10^{-6}$/°C.[17] In addition, the CTE values of residual glass phase $\alpha_g$, which were calculated by using Hormadaly's model[18] in our study, from Y1 to Y5 are $10.7 \times 10^{-6}$/°C, $10.4 \times 10^{-6}$/°C, $10.1 \times 10^{-6}$/°C, $9.2 \times 10^{-6}$/°C, and $9.1 \times 10^{-6}$/°C, respectively. As shown in Fig. 3, the theoretical value of CTE calculated by Eq. 2 is much closer to the experimental data compared with the Eq. 1. Thus, the modified formula Eq. 2 could be applied in this study.

Electrical properties of BABS glass–ceramics with various $Y_2O_3$ sintered at 920°C are listed in Table IV. The dielectric constant ($\varepsilon_r$) and loss ($\tan\delta$) are slightly increased from $6.1 \times 10^{-3}$ to $6.8 \times 10^{-3}$ and $3.2 \times 10^{-3}$ to $4.7 \times 10^{-3}$, respectively. This may be a result of the increase of resident glass phase and closed pores in glass. At the same time, the order of magnitude for the insulation resistivity is more than $10^{11}$ Ω cm for all specimens.

It is well known that the flexural strength and Young's modulus are the most important aspects in the mechanical properties of packaging materials. As shown in Fig. 4, the mechanical properties of BABS glass–ceramics strongly depend on the $Y_2O_3$ content. Both flexural strength and Young's modulus curves are closely correlated and exhibit a peak. Even a small amount of $Y_2O_3$ could remarkably improve the mechanical properties, that is, the flexural strength and Young's modulus is obviously enhanced from 140 MPa to 200 MPa and 56.5 GPa to 63.7 GPa, respectively. But the mechanical properties could be sharply reduced by adding an excessive $Y_2O_3$. Microcracking and internal stresses may play a crucial role. As we know, the displacive phase transition of β- to α-cristobalite with ~ 5% volume decrease would cause microcracks during the cooling stage.[15] Moreover, it has been proved that the thermal residual stress is generated during the cooling process due to the different CTE of each constituent phase.[19] With increasing $Y_2O_3$ content, the decrease of cristobalite content in the specimens will produce two effects. First, the reduction of microcracking could improve the strength. Second, the decrease of internal stress would lower strength. Meanwhile, the decrease in crystallinity will enhance the above two effects. For samples Y1–Y3, the slight decrease of cristobalite would not lead to the great reduction of internal stress. In this case, the first effect will act as the main factor to improve the strength significantly. However, for specimens Y4–Y5, the cristobalite content sharply declines from 11.5% to 3.6%, which will result in the obvious decrease of internal stress. Therefore, the second effect is the major reason to lower the strength dramatically.

The fractured section of BABS glass–ceramics with different amounts of $Y_2O_3$ sintered at 920°C was observed by SEM. As shown in Fig. 5, the rounded crystal phases (the dark gray regions) are evenly distributed throughout in the entire glass matrix (the light gray regions). It was observed that the distribution of grain size for samples Y1–Y3 (1–2 μm) is more uniform compared with samples Y4 and Y5 (0.5–2 μm). In addition, the glass matrix increased as the increase of $Y_2O_3$ addition to a certain degree, which is accordance with the crystallinity in Table II. Meanwhile, in order to clarify the composition of the residual glass and crystal, EDS analysis corresponding to two points of sample Y3 sintered at 920°C was made and the results are presented in Fig. 6. Boron, as a light element, cannot be detected by EDS. It indicates that point A with a large amount of silicon and oxygen could be quartz or cristobalite. And point B may correspond to the glass phase.

In order to understand the effect of $Y_2O_3$ addition on the sintering behavior of BABS glass–ceramics, the sintering kinetics of empirical formula Eq. 3 presented by Singh[20] was chosen.

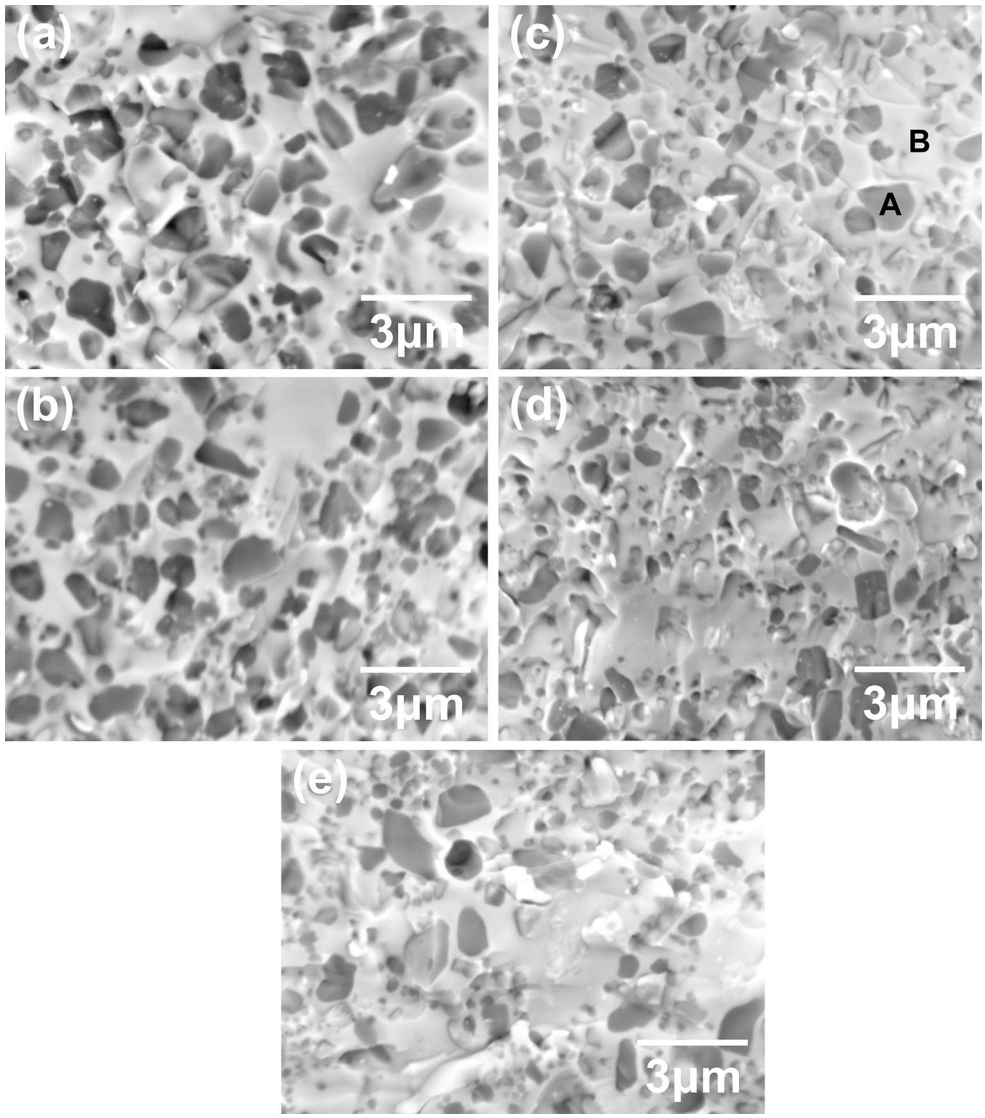


Fig. 5. SEM photographs for fractured specimens with different amounts of $Y_2O_3$ contents sintered at 920°C for 1 h (a) 0 wt.%, (b) 0.1 wt.%, (c) 0.2 wt.%, (d) 0.5 wt.%, (e) 1 wt.%.

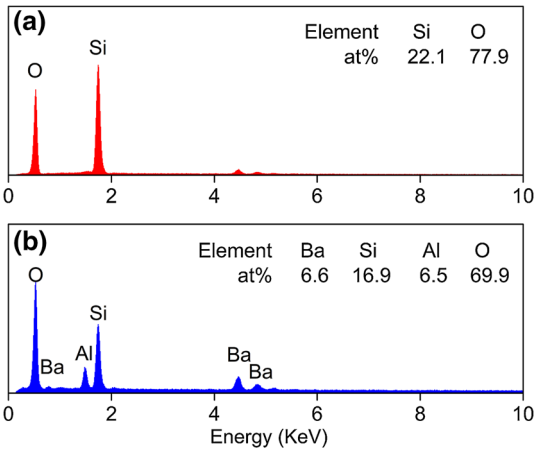


Fig. 6. EDS analysis of sample Y3 sintered at 920 (a) Spot A, (b) Spot B in Fig. 5c.

$$\lg \frac{dl}{l_0} = n \lg t + \lg k, \tag{3}$$

where $dl/l_0$ is the linear shrinkage rate, $t$ is holding time, $n$ is order of reaction, and $k$ is reaction rate constant. Therefore, if we could get the $k$ value, the activation energies of this study can be calculated by applying the Arrhenius equation via Eq. 4.

$$k = A \exp\left(-\frac{Q}{RT}\right), \tag{4}$$

where $k$ is the reaction rate constant, $Q$ represents the activation energy, $R$ is the universal gas constant, $T$ is the temperature, and $A$ is a constant.

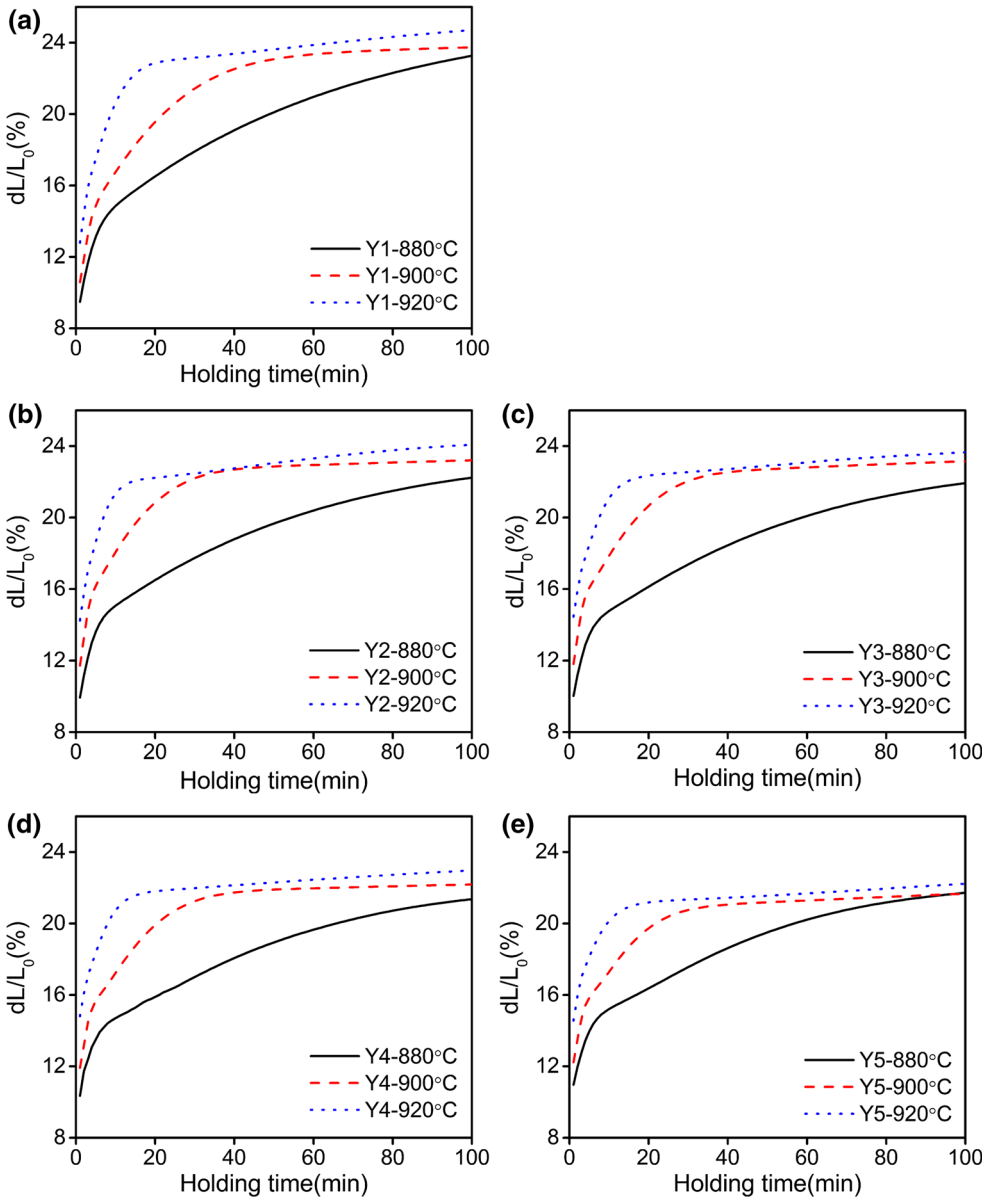


Fig. 7. Relation of BABS glass–ceramics linear shrinking rate with holding time at different sintering temperatures.

**Table V. The $k$ values for BABS glass–ceramics with various $Y_2O_3$ additions**

| | $k$ values | | | | |
|---|---|---|---|---|---|
| **Temperature (°C)** | **Y1** | **Y2** | **Y3** | **Y4** | **Y5** |
| 880 | 9.45 | 9.88 | 9.95 | 9.87 | 10.03 |
| 900 | 10.39 | 11.55 | 11.82 | 12.03 | 12.16 |
| 920 | 12.47 | 13.55 | 14.22 | 14.99 | 15.31 |

Figure 7 shows the relation between the linear shrinking rate and the holding time of BABS glass–ceramics at the varying sintering temperature of 880°C, 900°C, and 920°C, respectively. Data for the first few minutes were studied by plotting lg $(dl/l_0)$ versus lg $(t)$ to estimate the reaction rate constant $k$ in this system, and the results are given in Table V. So the activation energy $Q$ will be the slope of the plot of ln $k$ versus $1/T$ multiplied by the universal gas constant $R$. Accordingly, the change of

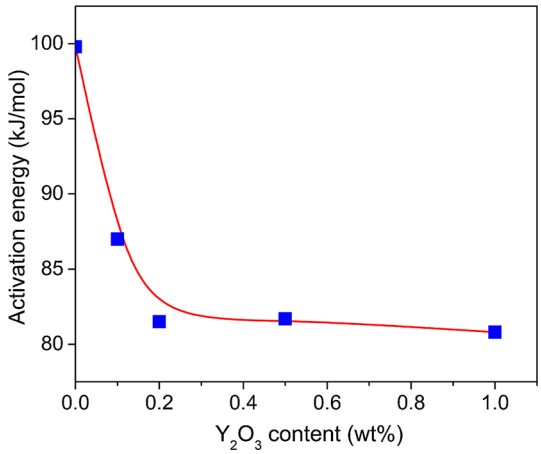


Fig. 8. Activation energy $Q$ versus $Y_2O_3$ content for sintering of BABS glass–ceramics.

activation energy $Q$ versus various $Y_2O_3$ is presented in Fig. 8. A small amount of $Y_2O_3$ addition could effectively reduce the sintering activation energy and promote the sintering procedure. However, the sintering activation energy would not change when $Y_2O_3$ content increased continuously. At these low $Y_2O_3$ levels, the most likely cause of viscosity increase is simply the lower crystallinity, i.e., more viscosity-enhancing $SiO_2$ retained in the glass. This may result in the decrease of the wettability of the liquid phase and hinder the sintering process.

## CONCLUSIONS

The influence of $Y_2O_3$ addition on the crystallization, thermal, mechanical, and electrical properties of $BaO$-$Al_2O_3$-$B_2O_3$-$SiO_2$ glass–ceramics was investigated. XRD analysis revealed that the major crystal phase was quartz, and the minor crystal phase was cristobalite. $Y_2O_3$ addition could inhibit the formation of cristobalite phase with a large CTE value, and, thus, the flexural strength and the Young's modulus increased remarkably. Moreover, the sintering kinetics demonstrated that the increase of $Y_2O_3$ content is favorable for promoting the sintering process of BABS, since the sintering activation energy decreased from 99.8 kJ/mol to 80.8 kJ/mol. BABS glass–ceramic with 0.2 wt.% $Y_2O_3$ sintered at 920°C exhibited excellent properties: a high flexural strength of 200 MPa, a high Young's modulus of 63.7 GPa, a suitable CTE value of $12.85 \times 10^{-6}$/°C, as well as a low dielectric constant of 6.5 and a low loss of $3.9 \times 10^{-3}$, which is a promising candidate for a CBGA package.

## REFERENCES

1. O. Dernovsek, A. Naeini, G. Preu, W. Wersing, M. Eberstein, and W.A. Schiller, *J. Eur. Ceram. Soc.* 21, 1693 (2001).
2. M.T. Sebastian and H. Jantunen, *Int. Mater. Rev.* 53, 57 (2008).
3. D. Nowak and A. Dziedzic, *Microelectron. Reliab.* 51, 1241 (2011).
4. K.S. Chin, C.C. Chang, C.H. Chen, Z. Guo, D. Wang, and W. Che, *IEEE Trans. Compon. Packag.* 4, 664 (2014).
5. B. Li, S. Wang, and Y. Fang, *J. Alloy. Compd.* 693, 9 (2017).
6. K. Wang, H. Yan, Z. Liang, and X. Cui, *Mater. Res. Bull.* 65, 249 (2015).
7. B. Li, B. Tang, and M. Xu, *J. Electron. Mater.* 27, 1 (2015).
8. E.S. Lim, B.S. Kim, J.H. Lee, and J.J. Kim, *J. Eur. Ceram. Soc.* 27, 825 (2007).
9. E.S. Lim, B.S. Kim, J.H. Lee, and J.J. Kim, *J. Electroceram.* 17, 359 (2006).
10. S. Chen and D. Zhu, *J. Alloy. Compd.* 536, 73 (2012).
11. A.I. Borhan, M. Gromada, G.G. Nedelcu, and L. Leontie, *Ceram. Int.* 42, 10459 (2016).
12. K. Singh, N. Gupta, and O.P. Pandey, *J. Mater. Sci.* 42, 6426 (2007).
13. V. Kumar, S. Sharma, O.P. Pandey, and K. Singh, *Solid State Ion.* 181, 79 (2010).
14. V. Kumar, O.P. Pandey, and K. Singh, *Ceram. Int.* 36, 1621 (2010).
15. O. Şan and C. Özgür, *J. Eur. Ceram. Soc.* 29, 2945 (2009).
16. A.A. Appen, *Silikattechnik* 5, 11 (1954).
17. P.W. McMillan, *Glass-Ceramics*, 2nd ed. (London: Academic, 1979).
18. J. Hormadaly, *J. Non Cryst. Solids* 79, 311 (1986).
19. Z. Huang, M. Gotoh, and Y. Hirose, *J. Mater. Process. Technol.* 209, 2446 (2009).
20. V.K. Singh, *J. Am. Ceram. Soc.* 64, C-133 (2006).